Using a phase-space cross section to study the structure of phase boundaries in large complex systems

2008 J. Phys. A: Math. Theor. 41 045101

(http://iopscience.iop.org/1751-8121/41/4/045101)

IOP PUBLISHING JOURNAL OF PHYSICS A: MATHEMATICAL AND THEORETICAL

J. Phys. A: Math. Theor. **41** (2008) 045101 (9pp) doi:10.1088/1751-8113/41/4/045101

Using a phase-space cross section to study the structure of phase boundaries in large complex systems

Gil Benkö and Henrik Jeldtoft Jensen

Institute for Mathematical Sciences, Imperial College London, 53 Prince's Gate, South Kensington Campus, London, SW7 2PG, UK
and
Department of Mathematics, Imperial College London, South Kensington Campus, SW7 2AZ, London, UK

E-mail: g.benkoe@imperial.ac.uk and h.jensen@imperial.ac.uk

Received 11 July 2007, in final form 16 November 2007
Published 15 January 2008
Online at stacks.iop.org/JPhysA/41/045101

Abstract
For large coupled nonlinear systems, it is difficult to visualize the high-dimensional phase space, which has been thoroughly studied in smaller systems with regard to phenomena such as riddled basins. Here, we propose a method to probe the phase space by defining a phase-space cross section. The method is applied to a system of dynamically coupled maps introduced by Ito and Kaneko (2001 *Phys. Rev. Lett.* **88** 028701, 2003 *Phys. Rev.* E **67** 046226). We show that the transitions between phases of different synchronization behaviour are not always sharp, but can be characterized by fractal boundaries in both phase and parameter space.

PACS number: 89.75.−k

1. Introduction

A hallmark of chaos in complex systems is sensitive dependence on initial conditions. An important property of the phase space of complex systems is basins of attraction, describing the sensitivity of the final state of a system depending on the initial conditions. In the case of riddled basins, multiple basins are present, intermingling in a fractal way and exacerbating this sensitivity (Alexander *et al* 1992, Ashwin *et al* 1996). However, properties of the phase space are difficult to study for large coupled nonlinear systems, as the phase space is high-dimensional and hard to visualize.

For instance, in this paper we are interested in studying large-scale synchronization, a dynamical property of networks that is widely observed in nature, for instance in the brain (Gray *et al* 1989, Varela *et al* 2001). Synchronization has been analysed for many physical systems (Pecora *et al* 1997, Pikovsky *et al* 2001), one model for synchronization is globally

coupled maps (GCM) (Ito and Kaneko 2001, Kaneko and Tsuda 2000), where the individual maps constituting the GCM have been extensively studied in dynamical systems research, especially the logistic map.

Here we propose a method to probe the phase space of such large systems by defining a phase-space cross section, allowing us to apply methods for the analysis of dynamical systems to large GCM. The aim is also to gain a better understanding of large network dynamics such as synchronization through these methods. Our main inspiration and focus is the nature of the boundaries between parameter regions of different behaviour in the model, detailed in the next section.

2. Model

We consider a GCM introduced by Ito and Kaneko (2001, 2003), where not only the maps but also the couplings between them are dynamical variables. This is closer to real-world systems, where connections are not always static but have their own dynamics. Thus in the GCM, there is a set of variables x^i, called units in the following, forming a network with connections of variable weights w^{ij}, related by

$$x_{n+1}^i = (1-c)f\left(x_n^i\right) + c\sum_{j=1}^{N} w_n^{ij} f\left(x_n^j\right) \tag{1}$$

$$f(x) = ax(1-x) \tag{2}$$

$$w_{n+1}^{ij} = \frac{\left[1+\delta g\left(x_n^i, x_n^j\right)\right]w_n^{ij}}{\sum_{j=1}^{N}\left[1+\delta g\left(x_n^i, x_n^j\right)\right]w_n^{ij}} \tag{3}$$

$$g(x, y) = 1 - 2|x - y|. \tag{4}$$

where a is the logistic equation parameter, and c is the coupling parameter. The function g defines a Hebbian update of the connection weights, by reinforcing a connection w^{ij} when the units x^i and x^j are similar. This function is scaled by δ, which controls the plasticity of the connection weights and is set to 0.1 throughout the present work. The dynamics of w^{ij} is normalized, dividing by $\sum_{j=1}^{N}\left[1+\delta g\left(x_n^i, x_n^j\right)\right]w_n^{ij}$ in order to avoid divergence, reflecting a limitation of the total weight of connections. The choice of initial conditions is the subject of the next sections. However, if not indicated otherwise, random initial conditions for the numerical simulations in the present work are defined as the initial x_0^i being randomly chosen from the uniform distribution between 0 and 1. The initial w_0^{ij} are set to 0 for $i = j$ and $1/(N-1)$ for $i \neq j$ throughout this work. We focus on the sensitivity on the initial x_0^i in this work. A preliminary study of the sensitivity on the choice of the initial w_0^{ij} indicated that it does not affect the results of this work; this will be studied at a later stage.

The system exhibits different long-term behaviours which are predominant in different parts of parameter space. In a simulation, all units may synchronize, forming one synchronized cluster containing all the units, or the set of units may be partitioned into subsets or clusters C_k within which there is synchronization or which contain single units not synchronized with any other unit. In line with Ito and Kaneko (2001, 2003), we will call the number of parts in this partition in the following the number of synchronized clusters. The number of synchronized clusters is then N if no synchronization at all occurs.

The connection strength w^{ij} between units in synchronized clusters C_k is around $1/N_{C_k}$. The connection strength between units in different synchronization clusters is vanishing (Ito and Kaneko 2003). This fact allows us to easily identify synchronized clusters.

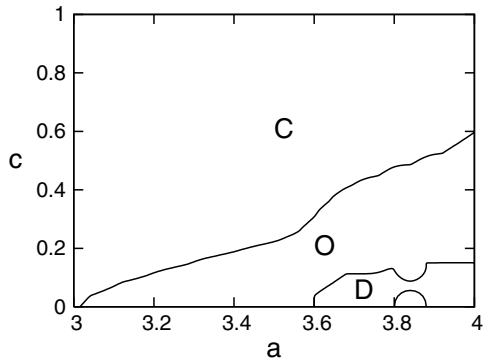

Figure 1. Schematic phase diagram of the GCM with $N = 100$ depending on parameters a and c, averaged over 500 samples. There are three phases: the coherent phase C, ordered phase O and disordered phase D. After (Ito and Kaneko 2001), see the text for a thorough explanation.

Figure 1 shows in a rough phase diagram which behaviour is predominant depending on a and c. The phase diagram is constructed by first simulating the system for 500 random initial conditions and 30 000 timesteps for each parameter pair (a, c). The resulting numbers of synchronized clusters were then averaged over the 500 runs for each (a, c). Three phases of predominant behaviour are now identified: in the coherent phase C, the average number of synchronization clusters is one, for all the 500 simulation runs all the units synchronize. In the disordered phase D, the average number of synchronization clusters is 100; for all the simulation runs no synchronization at all is achieved. The rest of the phase diagram is occupied by the ordered phase O. There the average number of synchronization clusters is strictly above 1 and strictly below 100; for all simulation runs, except for some close to the borders to D and C, there is always synchronization but only within parts of the set of units.

The structure of the phase O close to the borders to D and C is more complex. Indeed, we are especially interested in the transitions across the phase boundaries C/O and O/D (Peel and Jensen 2007), and will study them further in the next sections.

3. Phase-space cross section

We next examine this system using nonlinear system methods. We investigate the sensitive dependence of the final state on initial conditions near the phase boundaries. Pecora *et al* (1997) present studies on the synchronization of small chaotic systems based on stability analysis and bifurcation theory. For instance, an intriguing behaviour observed in GCM is riddled synchronization attractor basins. A basin is riddled when for every point in the basin a small error might lead to a different attractor; the two attractors are completely intermingled (Alexander *et al* 1992, Ashwin *et al* 1996). This is related to the concept of fractal basin boundaries (McDonald *et al* 1985, Takesue and Kaneko 1984), for which it suffices that the borders of two attractor basins are intermingled. This phenomenon is especially relevant and important regarding the final state of the system. The final state in physical systems with riddled basins is uncertain around these basin boundaries (Ott *et al* 1994, Pecora *et al* 1997).

However, we are interested in large systems, where it is not practicable to visualize the phase space in order to gain insight into its characteristics. Typically, in our studies the GCM is composed of 100 units.

We thus aim to sample a part of the phase space to make it amenable to our study of the boundaries C/O and O/D in the phase diagram. It is a first approach towards analysing the sensitive dependence on initial conditions in large systems.

Sampling algorithms applicable to sampling of the phase space include random sampling, orthogonal sampling and importance sampling (Ripley 1987). Random sampling is straightforward, random initial conditions as explained above were used to generate figure 1. Orthogonal sampling is similar and would involve partitioning the phase space into equal parts and selection of one random initial condition out of each part. Importance sampling samples from a distribution biased towards values that are more important in a given context, and subsequently corrects this bias. These methods do not sample contiguous parts of the phase space. However, we are interested in probing, for instance, the phase space at the boundaries C/O and O/D for fractal structure. Fractal structure such as fractal basin boundaries is revealed by studying the fine structure of the phase space and is not easily identified by looking at non-contiguous parts of the phase space. We found the method presented here was more efficient in picking up a difference between fractal and non-fractal basin boundaries. We thus use as a first step towards investigating the phase space of our system a contiguous one-dimensional curve through phase space. We want to tailor the shape of the curve to our system; it should take advantage of the symmetries of the system defined by (1) to (4). Thus the curve can be restricted to the part of the initial conditions for which $x_0^i \in [0, 0.5]$. The curve should also avoid the borders and diagonals of the phase space, where there is trivial synchronization.

There are obviously different ways of defining such a curve, but the probing by the curve can never be exhaustive except for a space filling curve, which is excluded for computational efficiency. We have examined different curve definitions but they do not seem to make an essential difference. We chose the following curve P for qualitative reasons as its definition is simple:

$$P = \left\{ \left(x_0^0 = \frac{1-\cos \pi t}{2}, \ldots x_0^i = \frac{i}{N-1}\frac{\sin \pi t}{2} + \frac{N-1-i}{N-1}\frac{1-\cos \pi t}{2}, \ldots x_0^{N-1} = \frac{\sin \pi t}{2} \right) \in \mathbb{R}^N \middle| t \in [0, 0.5] \right\}. \tag{5}$$

We calculate the outcome of simulating (1) to (4) as we change the initial conditions along P, keeping all control parameters (a, c, δ) constant, and we characterize the outcome by the number of synchronized clusters.

The variation of the number of synchronized clusters along P thus yields a one-dimensional cross section of the phase space, i.e. a probe of the appearance of the corresponding phase space.

An example of how we will represent the behaviour along P is shown for $a = 3.76$ and $c = 0.40$ in figure 2(a). The number of synchronized clusters is plotted with dots of different grey values against $t \in [0, 0.5]$, increasing with the number of synchronized clusters, from white (coherent) over grey (ordered) to black (disordered phase). We plot P by sampling initial conditions along P with a constant sampling step size of 0.001.

4. Results and discussion

Using the previously defined phase-space cross section, we can now study bigger systems, and extend the study of fractal basin boundaries to large GCM. For example, we can use the phase-space cross section P of figure 2(a) and calculate the fractal dimension of the boundary between the coherent and ordered regions in P, thus obtaining an insight into the nature of

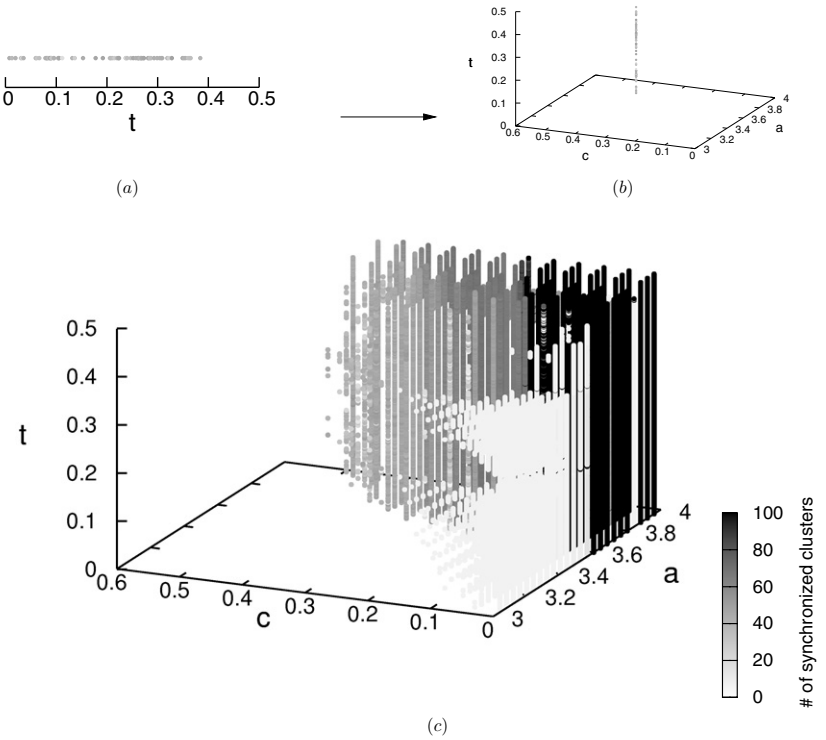

Figure 2. Expanding the phase diagram by the phase-space cross section. (*a*) The phase-space cross section for $a = 3.76$ and $c = 0.40$. The number of synchronized clusters is plotted against the parameter t of (5), going from white (coherent) over grey shades (ordered) to black (disordered phase). (*b*) The same phase-space cross section, placed along the t-axis in the space spanned by (a, c, t) on the line defined by $a = 3.76$ and $c = 0.40$. (*c*) Repeating the plotting of the previous phase-space cross section for and at every (a, c), thus obtaining a phase diagram in the space spanned by (a, c, t).

the boundary in the complete phase space. For example, the boundary between the coherent and ordered regions within P shown in figure 2(*a*) is Cantor set-like and has a box-counting dimension of $D_0 \approx 0.45$.

We will use the phase-space cross section in order to obtain a more detailed phase diagram of the GCM. We expand the GCM's phase diagram shown in figure 1, which is drawn in parameter space, by an additional dimension constructed from the phase space, the phase-space cross section. Figure 2(*b*) shows a phase-space cross section plotted perpendicularly to the (a, c) plane over the a and c parameter values it has been calculated for. In figure 2(*c*), we repeat this for each pair (a, c) and add all the phase-space cross sections perpendicularly to the (a, c) plane over their corresponding (a, c) values to obtain a more detailed phase diagram. The phase-space cross sections are constructed by sampling 500 initial conditions along P with a constant sampling step size of 0.001.

This process can be nicely illustrated by imagining it for the complex map $f_c(z) = z^2 + c$. In this case the phase space is just two-dimensional, spanned by $\mathrm{Re}(z)$, $\mathrm{Im}(z)$ and the behaviour in the phase space is described by a Julia set, varying for each c. The parameter space is also two-dimensional, spanned by $\mathrm{Re}(c)$, $\mathrm{Im}(c)$, and the behaviour is now described by the Mandelbrot set. The analogy to the more detailed phase diagram is obtained by adding a

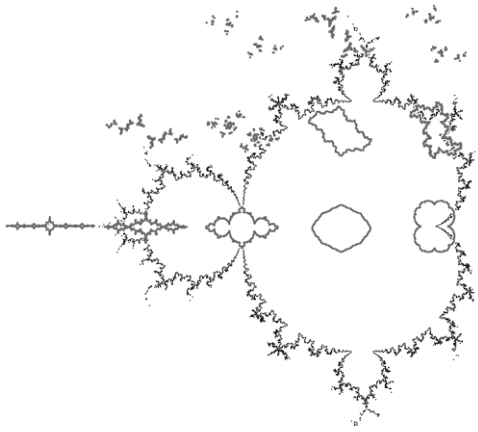

Figure 3. An 'extended phase diagram' of the complex map $f_c(z) = z^2 + c$. By superimposing on a sample of c values of the Mandelbrot set the corresponding Julia set, an analogous diagram to figure 2(c) is obtained.

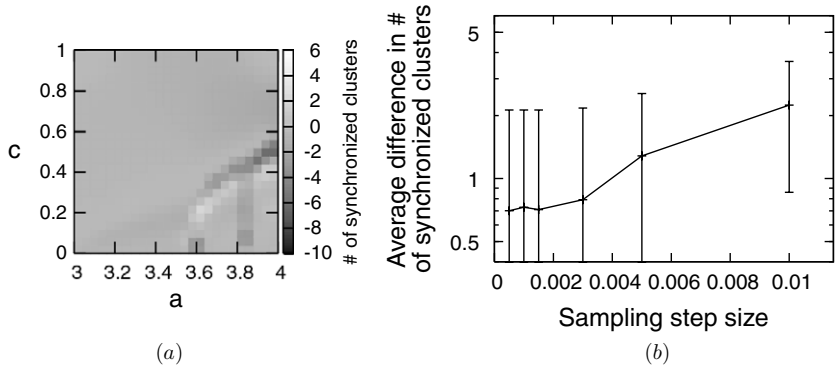

Figure 4. (a) Difference in number of synchronization clusters between phase diagrams obtained by random sampling and using P. (b) Average difference in the number of synchronized clusters between the phase diagrams obtained by random sampling and using P versus the sampling step size of P.

sketch of the corresponding Julia set to each or a sample of c values on the top of a Mandelbrot set (see figure 3).

The new extended phase diagram in figure 2(c) is similar to the diagram in figure 1. Every slice along the (a, c) plane in figure 2(c) is a regular phase diagram of the system for a single initial condition. Figure 7 shows an example for the initial condition corresponding to $t = 0.499$. Both in the regular and extended phase diagrams most of the parameter space is occupied by the coherent phase, while there are transitions into a first ordered, then disordered phase as a increases and c decreases. To appreciate how representative of the whole phase space P is, we average over the number of synchronized clusters in P for each (a, c) and compare it to the average over a random sample of 500 initial conditions for each (a, c). The result is shown in figure 4(a). The difference between the phase diagrams obtained by random

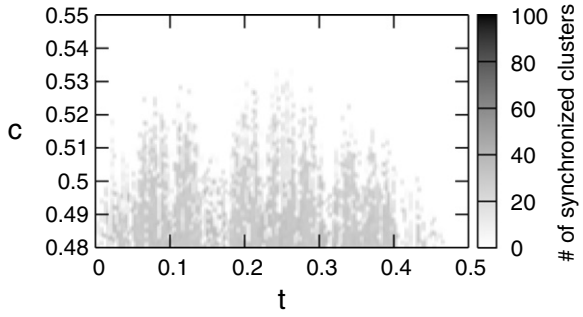

Figure 5. Plot of the phase-space cross section as a function of c.

sampling and using P is indeed small compared to $N = 100$. We repeated the calculation of the difference of phase diagrams for different sampling resolutions of P and show in figure 4(b) how the average difference in the number of synchronized clusters between the phase diagrams evolves with the sampling step size. As expected, the difference diminishes as the sampling step size becomes smaller. It seems, however, that the difference does not diminish further after the sampling step size falls below 0.0015. In the following, we will use a sampling step size of 0.0005.

A new feature visible in figure 2(c) and its slices as for example figure 7 is that the ordered phase O, shown in grey shades, is split into a light grey part I with values of a below $a_{\text{crit}} \approx 3.57$, which is the onset of chaos in the logistic map, and a dark grey part II with values of a above a_{crit}. In the former part, the behaviour of the $N = 100$ system is characterized by 2–6 synchronized clusters while in the latter part the system typically decomposes into 30–50 synchronized clusters. Also, the added dimension of the new phase diagram reveals that the boundaries of the phases are not simply smooth. The transition C/O_I is sharp, there is not an intermittent but a sudden change of phase at a threshold (a, c), which nevertheless varies smoothly along the phase-space cross section.

However, the boundary C/O_{II} seems to be fractal in both phase and parameter space. For more clarity, we can draw the phase-space cross section against the parameter c, with $a = 3.97$ for example, see figure 5. We observe indeed that as c increases from 0.45 to 0.55, the phase-space cross section changes from being completely in the ordered to completely in the coherent phase, going through a range where the cross section is alternating between the two phases in a fractal way, indicating a fractal basin boundary (McDonald *et al* 1985, Takesue and Kaneko 1984) in phase space. This is corroborated by finding more fine structure for higher plot resolutions.

As explained above, we can quantify the fractal nature of the boundaries in phase space by calculating the box-counting dimension D_0 of the boundary within the phase-space cross section (McDonald *et al* 1985). Figure 6(a) shows a detail of the phase diagram where the regions C, O_I, O_{II}, and D meet, around $a = 3.6$ and $c = 0.1$. Next to it, figure 6(b) shows the fractal dimension D_0 of the boundary between C, O_I, O_{II} and D within the phase-space cross section for each pair (a, c) in the considered part of the phase diagram. By comparing the phase and fractal dimension diagrams, we see that within the regions C, O_I, O_{II} of the phase diagram, $D_0 = 0$. Indeed, there the phase space and thus the phase-space cross section are 'filled' with one single region and contain no boundary. Where C and O_I meet, D_0 is also near 0. There the boundary within the phase-space cross section consists of a few points, and thus has theoretically a dimension of 0. However, where the regions C and O_{II} meet,

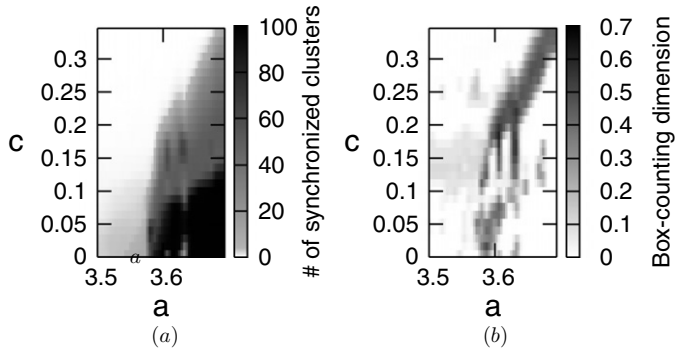

Figure 6. (*a*) Detail of the phase diagram of the GCM. (*b*) Box-counting dimension of the boundaries between regions C, O, and D within the phase-space cross section for each (a, c) in the phase diagram (*a*).

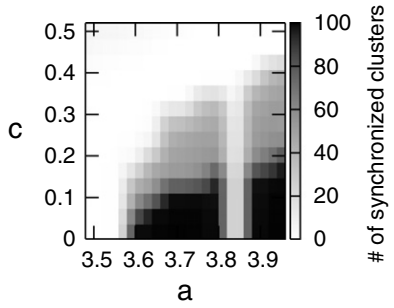

Figure 7. The slice corresponding to $t = 0.499$ of the extended phase diagram in figure 2(*c*).

$D_0 \approx 0.5$, quantifying the fractal nature of this border. The change of the C/O border from sharp (C/O_I) to fractal (C/O_{II}) is called a boundary metamorphosis (Grebogi *et al* 1987).

Most of the border O/D has $D_0 \approx 0$ and is not fractal, but for $a < 3.67$ D_0 increases up to values of 0.5. There is a lot of detail in this region which will be studied in future work.

The fractal nature of the boundaries in parameter space can be quantified as well, by calculating the box-counting dimension of the boundaries within the phase diagram and averaging over a sample of initial conditions. Thus if we calculate the dimension looking only at the boundaries C/O_I, C/O_{II}, O_I/D and O_{II}/D, we obtain almost always values near 1, except for C/O_{II} where $D_0 \approx 1.6$. Thus C/O_{II} is fractal in parameter space. As it was also the only fractal boundary in phase space, this indicates a correlation between the fractal nature in phase and parameter space, which has been partly proven for the complex map $f_c(z) = z^2 + c$ (Lei 1990).

Finally, a feature of the extended phase diagram in figure 2(*c*) is the small mixed coherent/ordered enclaves in the otherwise disordered phase, for example for $t \approx 0.5$, and $a \approx 3.85$, also seen in the slice, shown in figure 7, of the extended phase diagram corresponding to $t = 0.499$. This seems to indicate the advantage of using the phase-space cross section defined by (5), as follows. For $t \approx 0$ or $t \approx 0.5$, i.e. the beginning and end of P, the x_0^i values are close to each other, with $x_0^i \approx 0$ or $x_0^i \approx 0.5$ respectively. This allows probing into the behaviour of the system for almost synchronized initial conditions. Thus the small

mixed coherent/ordered enclaves in the otherwise disordered phase correspond to the islands of periodicity within the chaotic regime of an individual logistic map at $a \approx 3.85$, $a \approx 3.7, \ldots$. Thus we have an example where for almost synchronized initial conditions, the behaviour of the GCM is strongly influenced by the characteristics of the individual maps x^i.

5. Conclusion

In conclusion, we have constructed a tool for efficiently probing and further understanding the dynamics of networks of coupled maps, in this case the transitions between states of synchronization in a GCM. The phenomenon of fractal boundaries in phase and/or parameter space was found using this tool in the studied model, as suggested by previous findings in similar models (Lai and Winslow 1994), reviewed in Pecora *et al* (1997). The phase-space cross section can be generalized by defining similar P tailored to other systems. We have defined a similar phase-space cross section for a GCM analogous to the present work, based on the skewed tent map instead of the logistic map. The preliminary results obtained were similar to the results of the present work.

One example for the relevance of the synchronization observed in GCM is neural networks. There is evidence that the elementary cognitive acts underlying cognition are achieved by transient neural assemblies dynamically linked by synchronization (Varela *et al* 2001). Studying phases is thus important in the context of analysing mental states. For example, a riddled phase space might potentially facilitate switching between disordered dynamics in a neural network and the emergence of synchronized assemblies.

Acknowledgments

Useful discussions with Adele Peel, computer support by Andy Thomas and the use of the Imperial College High Performance Computing Service are gratefully acknowledged.

References

Alexander J C, Kan I, Yorke J A and You Z 1992 *Int. J. Bifurcation Chaos Appl. Sci. Eng.* **2** 795–813
Ashwin P, Buescu J and Stewart I 1996 *Nonlinearity* **9** 703–37
Gray C, Konig P, Engel A and Singer W 1989 *Nature* **338** 334–7
Grebogi C, Ott E and Yorke J 1987 *Physica* D **24** 243–62
Ito J and Kaneko K 2001 *Phys. Rev. Lett.* **88** 028701
Ito J and Kaneko K 2003 *Phys. Rev.* E **67** 046226
Kaneko K and Tsuda I 2000 *Complex Systems: Chaos and Beyond. A Constructive Approach with Applications in Life Sciences* (Berlin: Springer)
Lai Y C and Winslow R 1994 *Phys. Rev. Lett.* **72** 164–7
Lei T 1990 *Commun. Math. Phys.* **134** 587–617
McDonald S W, Grebogi C, Ott E and Yorke J A 1985 *Physica* D **17** 125–53
Ott E, Alexander J C, Kan I, Sommerer J C and Yorke J A 1994 *Physica* D **76** 384–410
Pecora L, Carroll T, Johnson G, Mar D and Heagy J 1997 *Chaos* **7** 520–43
Peel A and Jensen H J 2007 *Preprint* cond-mat/0703804v1
Pikovsky A, Rosenblum M and Kurths J 2001 *Synchronization: A Universal Concept in Nonlinear Sciences (Cambridge Nonlinear Science Series)* (Cambridge: Cambridge University Press)
Ripley B D 1987 *Stochastic Simulation* (New York: Wiley)
Takesue S and Kaneko K 1984 *Prog. Theor. Phys.* **71** 35–49
Varela F, Lachaux J P, Rodriguez E and Martinerie J 2001 *Nature Rev. Neurosci.* **2** 229–39